









# TECH BRIEFS

NATIONAL AERONAUTICS AND SPACE ADMINISTRATION

-  **Technology Focus**
-  **Electronics/Computers**
-  **Software**
-  **Materials**
-  **Mechanics/Machinery**
-  **Manufacturing**
-  **Bio-Medical**
-  **Physical Sciences**
-  **Information Sciences**
-  **Books and Reports**



## INTRODUCTION

Tech Briefs are short announcements of innovations originating from research and development activities of the National Aeronautics and Space Administration. They emphasize information considered likely to be transferable across industrial, regional, or disciplinary lines and are issued to encourage commercial application.

### Additional Information on NASA Tech Briefs and TSPs

Additional information announced herein may be obtained from the NASA Technical Reports Server: <http://ntrs.nasa.gov>.

Please reference the control numbers appearing at the end of each Tech Brief. Information on NASA's Innovative Partnerships Program (IPP), its documents, and services is available on the World Wide Web at <http://www.ipp.nasa.gov>.

Innovative Partnerships Offices are located at NASA field centers to provide technology-transfer access to industrial users. Inquiries can be made by contacting NASA field centers listed below.

## NASA Field Centers and Program Offices

### Ames Research Center

David Morse  
(650) 604-4724  
[david.r.morse@nasa.gov](mailto:david.r.morse@nasa.gov)

### Dryden Flight Research Center

Ron Young  
(661) 276-3741  
[ronald.m.young@nasa.gov](mailto:ronald.m.young@nasa.gov)

### Glenn Research Center

Kimberly A. Dalgleish-Miller  
(216) 433-8047  
[kimberly.a.dalgleish@nasa.gov](mailto:kimberly.a.dalgleish@nasa.gov)

### Goddard Space Flight Center

Nona Cheeks  
(301) 286-5810  
[nona.k.cheeks@nasa.gov](mailto:nona.k.cheeks@nasa.gov)

### Jet Propulsion Laboratory

Indrani Graczyk  
(818) 354-2241  
[indrani.graczyk@jpl.nasa.gov](mailto:indrani.graczyk@jpl.nasa.gov)

### Johnson Space Center

John E. James  
(281) 483-3809  
[john.e.james@nasa.gov](mailto:john.e.james@nasa.gov)

### Kennedy Space Center

David R. Makufka  
(321) 867-6227  
[david.r.makufka@nasa.gov](mailto:david.r.makufka@nasa.gov)

### Langley Research Center

Michelle Ferebee  
(757) 864-5617  
[michelle.t.ferebee@nasa.gov](mailto:michelle.t.ferebee@nasa.gov)

### Marshall Space Flight Center

Terry L. Taylor  
(256) 544-5916  
[terry.taylor@nasa.gov](mailto:terry.taylor@nasa.gov)

### Stennis Space Center

Ramona Travis  
(228) 688-3832  
[ramona.e.travis@ssc.nasa.gov](mailto:ramona.e.travis@ssc.nasa.gov)

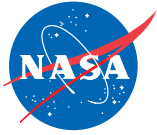
### NASA Headquarters

Daniel Lockney,  
Technology Transfer Program Executive  
(202) 358-2037  
[daniel.p.lockney@nasa.gov](mailto:daniel.p.lockney@nasa.gov)

### Small Business Innovation Research (SBIR) & Small Business Technology Transfer (STTR) Programs

Rich Leshner, Program Executive  
(202) 358-4920  
[rleshner@nasa.gov](mailto:rleshner@nasa.gov)





# TECH BRIEFS

NATIONAL AERONAUTICS AND SPACE ADMINISTRATION



## 5 Technology Focus: Electronic Components

- 5 Pattern Generator for Bench Test of Digital Boards
- 5 670-GHz Down- and Up-Converting HEMT-Based Mixers
- 6 Lidar Electro-Optic Beam Switch with a Liquid Crystal Variable Retarder
- 6 Feedback Augmented Sub-Ranging (FASR) Quantizer
- 7 Real-Time Distributed Embedded Oscillator Operating Frequency Monitoring



## 9 Software

- 9 Software Modules for the Proximity-1 Space Link Interleaved Time Synchronization (PITS) Protocol
- 9 Description and User Instructions for the Quaternion\_to\_orbit\_v3 Software
- 9 AdapChem
- 9 Mars Relay Lander and Orbiter Overflight Profile Estimation
- 10 Extended Testability Analysis Tool
- 10 Interactive 3D Mars Visualization
- 10 Rapid Diagnostics of Onboard Sequences
- 11 MER Telemetry Processor
- 11 pyam: Python implementation of YaM



## 13 Manufacturing & Prototyping

- 13 Process for Patterning Indium for Bump Bonding
- 13 Archway for Radiation and Micrometeorite Occurrence Resistance



## 15 Physical Sciences

- 15 4D Light Field Imaging System Using Programmable Aperture
- 15 Device and Container for Reheating and Sterilization

- 16 Radio Frequency Plasma Discharge Lamps for Use as Stable Calibration Light Sources
- 17 Membrane Shell Reflector Segment Antenna
- 17 High-Speed Transport of Fluid Drops and Solid Particles via Surface Acoustic Waves
- 18 Compact Autonomous Hemispheric Vision System
- 19 A Distributive, Non-Destructive, Real-Time Approach to Snowpack Monitoring



## 21 Bio-Medical

- 21 Wideband Single-Crystal Transducer for Bone Characterization



## 23 Information Technology

- 23 Numerical Simulation of Rocket Exhaust Interaction With Lunar Soil
- 23 Motion Imagery and Robotics Application (MIRA): Standards-Based Robotics
- 24 Particle Filtering for Model-Based Anomaly Detection in Sensor Networks



## 27 Books & Reports

- 27 Ka-band Digitally Beamformed Airborne Radar Using SweepSAR Technique
- 27 Composite With *In Situ* Plenums
- 27 Multi-Beam Approach for Accelerating Alignment and Calibration of HypsIRI-Like Imaging Spectrometers
- 27 JWST Lifting System
- 27 Next-Generation Tumbleweed Rover
- 28 Pneumatic System for Concentration of Micrometer-Size Lunar Soil

This document was prepared under the sponsorship of the National Aeronautics and Space Administration. Neither the United States Government nor any person acting on behalf of the United States Government assumes any liability resulting from the use of the information contained in this document, or warrants that such use will be free from privately owned rights.





## Pattern Generator for Bench Test of Digital Boards

**Fresh data is streamed continuously for many tens of seconds with no gaps at 40 MHz.**

*NASA's Jet Propulsion Laboratory, Pasadena, California*

All efforts to develop electronic equipment reach a stage where they need a board test station for each board. The SMAP digital system consists of three board types that interact with each other using interfaces with critical timing. Each board needs to be tested individually before combining into the integrated digital electronics system. Each board needs critical timing signals from the others to be able to operate. A bench test system was developed to support test of each board. The test system produces all the outputs of the control and timing unit, and is delivered much earlier than the timing unit.

Timing signals are treated as data. A large file is generated containing the state of every timing signal at any instant. This file is streamed out to an IO card, which is wired directly to the device-under-test (DUT) input pins. This provides a flexible test environment that can be adapted to any of the boards required to test in a standalone configuration. The problem of generating the critical timing signals is then transferred from a hardware problem

to a software problem where it is more easily dealt with.

The first board to be tested was the ADC Digital Processor board (ADP). The ADP needed a complex Xilinx configuration data stream to operate, plus timing signals. The IO card is wired directly to the configuration and timing inputs of the board through VME connectors. A slower pattern maker program combines the Xilinx configuration and desired timing into a large data file. This data file is clocked out at 40 MHz (32 bits of data) into 28 inputs of the ADP to make it run.

The formatter board needs data from an ADP, plus timing information from the control and timing unit. Data captured from the ADP in its standalone test is combined with timing information into a large file. The large file streams out the IO card and is wired to formatter inputs. Since the formatter has more inputs than the IO card has bits, several signals were cross-strapped (duplicated), making it appear to the formatter that it was receiving two ADP boards when it was in fact receiving two

copies of the same ADP board. In combined ADP/formatter integration, the IO card emulates the timing unit only.

Using IO cards to emulate missing hardware for bench test is an older technology. The improvement here is the ability to stream out fresh data continuously for many tens of seconds with no gaps at 40 MHz. This allows precise control over timing with time tag information that varies over a wide range. This allows a much better bench test than would have been possible in short pulses.

By allowing more complete testing of the individual boards when they are ready rather than deferring test to integration, the delivery of the SMAP digital system is accelerated.

*This work was done by Andrew C. Berkun and Anhua J. Chu of Caltech for NASA's Jet Propulsion Laboratory. Further information is contained in a TSP (see page 1).*

*The software used in this innovation is available for commercial licensing. Please contact Daniel Broderick of the California Institute of Technology at [danielb@caltech.edu](mailto:danielb@caltech.edu). Refer to NPO-48231.*

## 670-GHz Down- and Up-Converting HEMT-Based Mixers

**Applications include passive, active, or radar imaging.**

*NASA's Jet Propulsion Laboratory, Pasadena, California*

A large category of scientific investigation takes advantage of the interactions of signals in the frequency range from 300 to 1,000 GHz and higher. This includes astronomy and atmospheric science, where spectral observations in this frequency range give information about molecular abundances, pressures, and temperatures of small-sized molecules such as water. Additionally, there is a minimum in the atmospheric absorption at around 670 GHz that makes this frequency useful for terrestrial imaging, radar, and possibly communications purposes. This is because 670 GHz is a good compromise for imaging and

radar applications between spatial resolution (for a given antenna size) that favors higher frequencies, and atmospheric losses that favor lower frequencies. A similar trade-off applies to communications link budgets: higher frequencies allow smaller antennas, but incur a higher loss.

All of these applications usually require converting the RF (radio frequency) signal at 670 GHz to a lower IF (intermediate frequency) for processing. Further, transmitting for communication and radar generally requires up-conversion from IF to the RF. The current state-of-the-art device for per-

forming the frequency conversion is based on Schottky diode mixers for both up and down conversion in this frequency range for room-temperature operation. Devices that can operate at room temperature are generally required for terrestrial, military, and planetary applications that cannot tolerate the mass, bulk, and power consumption of cryogenic cooling.

The technology has recently advanced to the point that amplifiers in the region up to nearly 1,000 GHz are feasible. Almost all of these have been based on indium phosphide pseudomorphic high-electron mobility transis-

tors (pHEMTs), in the form of monolithic microwave integrated circuits (MMICs). Since the processing of HEMT amplifiers is quite different from that of Schottky diodes, use of Schottky mixers requires separate MMICs for the mixers and amplifiers. Fabrication of all the down-/up-conversion circuitry on single MMICs, using all-HEMT circuits, would constitute a major advance in circuit simplicity.

Three pHEMT-based subharmonic 670-GHz mixers were developed that are all subharmonically pumped at about 300 GHz, which greatly simplifies the local oscillator (LO) source, compared to a fundamentally pumped mixer requiring a 600-GHz source. The mixers use an active topology. Fundamentally, they are configured as a single-stage, grounded-source amplifier with a drain load controlled by the LO. The drain load is an additional transistor, or pair of transistors, switched by the LO signal.

This effectively samples the signal from the amplifier at the LO frequency, and passes the beat note on to the output terminal of the mixer.

In the down-converting mixer, the 670-GHz RF input is connected to the gate of the grounded source stage, whose drain is directly connected to the source or sources of the LO FETs (field-effect transistors). One version has only a single transistor in the drain load, and relies on the non-linearity of the FET plus the output tuning circuitry to block the RF and LO signals and passes only the IF to the output terminal.

The second down-converting mixer replaces the single LO FET with a pair having sources and drains connected together. The LO signal is fed to the two gates through a network that gives a 180° phase shift to one FET. Hence, the two FETs are switched on for alternating half-cycles of the 300-GHz LO, and the

drain FET pair acts like a sampler at twice the LO frequency. Simulations indicate about 6 dB of improvement in the conversion gain, from -6 dB for the two-FET design to around 0 dB for the three-FET design.

For the up-converting mixer, the circuit is similar to the three-FET down-converter, but with the IF input going to the gate of the grounded source stage, and the RF output taken from the drains of the LO transistors. The RF and IF matching networks are also modified to the correct frequency ranges. Simulations indicate a conversion gain of about 3 dB.

*This work was done by Erich T. Schlecht, Goutam Chattopadhyay, Robert H. Lin, and Seth Sin of Caltech; and William Deal, Bryan Rodriguez, Brian Bayuk, Kevin Leong, and Gerry Mei of Northrup Grumman for NASA's Jet Propulsion Laboratory. Further information is contained in a TSP (see page 1). NPO-48204*

---

## Lidar Electro-Optic Beam Switch with a Liquid Crystal Variable Retarder

*Lyndon B. Johnson Space Center, Houston, Texas*

A document discusses a liquid crystal variable retarder, an electro-optic element that changes the polarization of an optical beam in response to a low-voltage electronic signal. This device can be fabricated so that the element creates, among other states, a half-wave of retardance that can be reduced to a very small retardance. When aligned to a po-

larized source, this can act to rotate the polarization by 90° in one state, but generate no rotation in the other state. If the beam is then incident on a polarization beam splitter, it will efficiently switch from one path to the other when the voltage is applied. The laser beam switching system has no moving parts, improving reliability over mechanical

switching. It is low cost, tolerant of high laser power density, and needs only simple drive electronics, minimizing the required system resources.

*This work was done by James Baer of Ball Aerospace & Technologies Corp. for Johnson Space Center. Further information is contained in a TSP (see page 1). MSC-25113-1*

---

## Feedback Augmented Sub-Ranging (FASR) Quantizer

**This device increases the accuracy of a switched capacitor amplifier, reduces the power and area of an integrated circuit, and reduces manufacturing cost.**

*Goddard Space Flight Center, Greenbelt, Maryland*

This innovation is intended to reduce the size, power, and complexity of pipeline analog-to-digital converters (ADCs) that require high resolution and speed along with low power. Digitizers are important components in any application where analog signals (such as light, sound, temperature, etc.) need to be digitally processed. The innovation implements amplification of a sampled residual voltage in a switched capacitor amplifier stage that does not

depend on charge redistribution. The result is less sensitive to capacitor mismatches that cause gain errors, which are the main limitation of such amplifiers in pipeline ADCs. The residual errors due to mismatch are reduced by at least a factor of 16, which is equivalent to at least 4 bits of improvement. The settling time is also faster because of a higher feedback factor.

In traditional switched capacitor residue amplifiers, closed-loop amplifi-

cation of a sampled and held residue signal is achieved by redistributing sampled charge onto a feedback capacitor around a high-gain transconductance amplifier. The residual charge that was sampled during the acquisition or sampling phase is stored on two or more capacitors, often equal in value or integral multiples of each other. During the hold or amplification phase, all of the charge is redistributed onto one capacitor in the feedback loop of the ampli-



fier to produce an amplified voltage. The key error source is the non-ideal ratios of feedback and input capacitors caused by manufacturing tolerances, called "mismatches." The mismatches cause non-ideal closed-loop gain, leading to higher differential non-linearity. Traditional solutions to the mismatch errors are to use larger capacitor values (than dictated by thermal noise re-

quirements) and/or complex calibration schemes, both of which increase the die size and power dissipation.

The key features of this innovation are (1) the elimination of the need for charge redistribution to achieve an accurate closed-loop gain of two, (2) a higher feedback factor in the amplifier stage giving a higher closed-loop bandwidth compared to the prior art, and

(3) reduced requirement for calibration. The accuracy of the new amplifier is mainly limited by the sampling networks' parasitic capacitances, which should be minimized in relation to the sampling capacitors.

*This work was done by Gerard Quilligan of Goddard Space Flight Center. Further information is contained in a TSP (see page 1).GSC-16187-1*

---

## Real-Time Distributed Embedded Oscillator Operating Frequency Monitoring

*Lyndon B. Johnson Space Center, Houston, Texas*

A document discusses the utilization of embedded clocks inside of operating network data links as an auxiliary clock source to satisfy local oscillator monitoring requirements. Modern network interfaces, typically serial network links, often contain embedded clocking information of very tight precision to recover data from the link. This embedded clocking data can be utilized by the receiving device to monitor the local oscillator for tolerance to required specifications, often important in high-integrity fault-tolerant applications.

A device can utilize a received embedded clock to determine if the local or the remote device is out of tolerance by using a single link. The local device can determine if it is failing, assuming a single fault model, with two or more active links. Network fabric components, containing

many operational links, can potentially determine faulty remote or local devices in the presence of multiple faults.

Two methods of implementation are described. In one method, a recovered clock can be directly used to monitor the local clock as a direct replacement of an external local oscillator. This scheme is consistent with a general clock monitoring function whereby clock sources are clocking two counters and compared over a fixed interval of time. In another method, overflow/underflow conditions can be used to detect clock relationships for monitoring. These network interfaces often provide clock compensation circuitry to allow data to be transferred from the received (network) clock domain to the internal clock domain. This circuit could be modified to detect overflow/underflow conditions of the

buffering required and report a fast or slow receive clock, respectively.

*This work was done by Julie Pollock, Brett Oliver, and Christopher Brickner of Honeywell, Inc. for Johnson Space Center. For further information, contact the JSC Innovation Partnerships Office at (281) 483-3809.*

*Title to this invention has been waived under the provisions of the National Aeronautics and Space Act {42 U.S.C. 2457(f)}, to Honeywell, Inc. Inquiries concerning licenses for its commercial development should be addressed to:*

*Aerospace – Defense & Space  
Honeywell  
P.O. Box 52199  
Phoenix, AZ 85072-2199  
Phone No.: (602) 822-3000*

*Refer to MSC-24765-1, volume and number of this NASA Tech Briefs issue, and the page number.*





## Software Modules for the Proximity-1 Space Link Interleaved Time Synchronization (PITS) Protocol

The Proximity-1 Space Link Interleaved Time Synchronization (PITS) protocol provides time distribution and synchronization services for space systems. A software prototype implementation of the PITS algorithm has been developed that also provides the test harness to evaluate the key functionalities of PITS with simulated data source and sink.

PITS integrates time synchronization functionality into the link layer of the CCSDS Proximity-1 Space Link Protocol. The software prototype implements the network packet format, data structures, and transmit- and receive-timestamp function for a time server and a client. The software also simulates the transmit and receive-time stamp exchanges via UDP (User Datagram Protocol) socket between a time server and a time client, and produces relative time offsets and delay estimates.

*This work was done by Simon S. Woo, John R. Veregge, Jay L. Gao, and Loren P. Clare of Caltech; and David Mills of the University of Delaware for NASA's Jet Propulsion Laboratory. For more information, contact [iaoffice@jpl.nasa.gov](mailto:iaoffice@jpl.nasa.gov).*

*This software is available for commercial licensing. Please contact Daniel Broderick of the California Institute of Technology at [danielb@caltech.edu](mailto:danielb@caltech.edu). Refer to NPO-47404.*

## Description and User Instructions for the Quaternion\_to\_orbit\_v3 Software

For a given inertial frame of reference, the software combines the spacecraft orbits with the spacecraft attitude quaternions, and rotates the body-fixed reference frame of a particular spacecraft to the inertial reference frame. The conversion assumes that the two spacecraft are aligned with respect to the mutual line of sight, with a parameterized time tag. The software is implemented in Python and is completely open source. It is very versatile, and may be applied under various circumstances and for other related purposes. Based on the solid linear algebra analysis, it has an extra option for compensating the linear pitch.

This software has been designed for simulation of the calibration maneuvers performed by the two spacecraft comprising the GRAIL mission to the Moon, but has potential use for other applications. In simulations of formation flights, one needs to coordinate the spacecraft orbits represented in an appropriate inertial reference frame and the spacecraft attitudes. The latter are usually given as the time series of quaternions rotating the body-fixed reference frame of a particular spacecraft to the inertial reference frame. It is often desirable to simulate the same maneuver for different segments of the orbit. It is also useful to study various maneuvers that could be performed at the same orbit segment. These two lines of study are more time- and labor-efficient if the attitude and orbit data are generated independently, so that the part of the data that has not been changed can be “recycled” in the course of multiple simulations.

*This work was done by Dmitry V. Strelakov, Gerhard L. Kruizinga, Meegyeong Paik, Dah-Ning Yuan, and Sami W. Asmar of Caltech for NASA's Jet Propulsion Laboratory. Further information is contained in a TSP (see page 1).*

*This software is available for commercial licensing. Please contact Daniel Broderick of the California Institute of Technology at [danielb@caltech.edu](mailto:danielb@caltech.edu). Refer to NPO-47701.*

## AdapChem

AdapChem software enables high efficiency, low computational cost, and enhanced accuracy on computational fluid dynamics (CFD) numerical simulations used for combustion studies. The software dynamically allocates smaller, reduced chemical models instead of the larger, full chemistry models to evolve the calculation while ensuring the same accuracy to be obtained for steady-state CFD reacting flow simulations.

The software enables detailed chemical kinetic modeling in combustion CFD simulations. AdapChem adapts the reaction mechanism used in the CFD to the local reaction conditions. Instead of a single, comprehensive reaction mechanism throughout the computation, a dynamic distribution of smaller, reduced models is used to capture accurately the chemical kinetics at a fraction of the cost of the tradi-

tional “single-mechanism” approach.

*This work was done by Oluwayemisi O. Oluwole and Hsi-Wu Wong of Aerodyne Research Inc., and William Green of MIT for Glenn Research Center. Further information is contained in a TSP (see page 1).*

*Inquiries concerning rights for the commercial use of this invention should be addressed to NASA Glenn Research Center, Innovative Partnerships Office, Attn: Steven Fedor, Mail Stop 4-8, 21000 Brookpark Road, Cleveland, Ohio 44135. Refer to LEW-18786-1.*

## Mars Relay Lander and Orbiter Overflight Profile Estimation

This software allows science and mission operations to view graphs of geometric overflights of satellites and landers within the Mars (or other planetary) networks. It improves on the MaROS Web interface within any modern Web browser, in that it adds new capabilities to the MaROS suite.

The profile for an overflight is an important element for selecting communication/overflight opportunities between the landers and orbiters within the Mars network. Unfortunately, determining these estimates is very computationally expensive and difficult to compute by hand. This software allows the user to select different overflights (via the existing MaROS Web interface) and specify the smoothness of the estimation.

Estimates for the geometric relationship between a lander and an orbiter are determined based upon the orbital conditions of the orbiter at the moment the orbiter rises above the horizon from the perspective of the lander. It utilizes 2-body orbital equations to propagate the trajectory through the duration of the view period, and returns profiles that represent the range between the two vehicles, and the elevation and azimuth angles of the orbiter as measured from the lander's position. The algorithms assume a 2-body relationship with an ideal, spherical planetary body, so therefore can see errors less than 2% at polar landing sites on Mars. These algorithms are being implemented to provide rough estimates rapidly for the geometry of a geometric view period where more complete data is unavailable, such as for

planning purposes.

While other software for this task exists, each at the time of this reporting has been contained within a much more complicated package. This tool allows science and mission operations to view the estimates with a few clicks of the mouse.

*This work was done by Michael N. Wallick, Daniel A. Allard, Roy E. Gladden, and Corey L. Peterson of Caltech for NASA's Jet Propulsion Laboratory. Further information is contained in a TSP (see page 1).*

*This software is available for commercial licensing. Please contact Daniel Broderick of the California Institute of Technology at [danielb@caltech.edu](mailto:danielb@caltech.edu). Refer to NPO-47722.*

---

## Extended Testability Analysis Tool

The Extended Testability Analysis (ETA) Tool is a software application that supports fault management (FM) by performing testability analyses on the fault propagation model of a given system. Fault management includes the prevention of faults through robust design margins and quality assurance methods, or the mitigation of system failures. Fault management requires an understanding of the system design and operation, potential failure mechanisms within the system, and the propagation of those potential failures through the system.

The purpose of the ETA Tool software is to process the testability analysis results from a commercial software program called TEAMS Designer in order to provide a detailed set of diagnostic assessment reports. The ETA Tool is a command-line process with several user-selectable report output options. The ETA Tool also extends the COTS testability analysis and enables variation studies with sensor sensitivity impacts on system diagnostics and component isolation using a single testability output. The ETA Tool can also provide extended analyses from a single set of testability output files.

The following analysis reports are available to the user: (1) the Detectability Report provides a breakdown of how each tested failure mode was detected, (2) the Test Utilization Report identifies all the failure modes that each test detects, (3) the Failure Mode Isolation Report demonstrates the system's ability to discriminate between failure modes, (4) the Component Isolation Report demonstrates the system's ability to discriminate between failure modes relative to the components containing the failure modes, (5) the Sen-

sor Sensitivity Analysis Report shows the diagnostic impact due to loss of sensor information, and (6) the Effect Mapping Report identifies failure modes that result in specified system-level effects.

The ETA Tool provides iterative assessment analyses for conducting sensor sensitivity studies, as well as a command-line option that allows the user to specify the component isolation level. The tool accesses system design information from the diagnostic model to generate detailed diagnostic assessment reports, and command-line processing enables potential batch mode processing of TEAMS Designer models. The tool also features user-specified report options that include internal source calls and access to system environmental variables – features that enable automation of the previously labor-intensive manipulation of input files. The software generates detailed, readable diagnostic assessment reports that can be viewed in an Internet browser or imported into either Microsoft Word or Excel programs. Procedural C code provides fast, consistent, and efficient processing of the diagnostic model information.

*This work was done by Kevin Melcher of Glenn Research Center, and William A. Maul and Christopher Fulton of QinetiQ North America. Further information is contained in a TSP (see page 1).*

*Inquiries concerning rights for the commercial use of this invention should be addressed to NASA Glenn Research Center, Innovative Partnerships Office, Attn: Steven Fedor, Mail Stop 4-8, 21000 Brookpark Road, Cleveland, Ohio 44135. Refer to LEW-18795-1.*

---

## Interactive 3D Mars Visualization

The Interactive 3D Mars Visualization system provides high-performance, immersive visualization of satellite and surface vehicle imagery of Mars. The software can be used in mission operations to provide the most accurate position information for the Mars rovers to date. When integrated into the mission data pipeline, this system allows mission planners to view the location of the rover on Mars to 0.01-meter accuracy with respect to satellite imagery, with dynamic updates to incorporate the latest position information. Given this information so early in the planning process, rover drivers are able to plan more accurate drive activities for the rover than ever before, increasing the execution of science activities significantly. Scientifically, this 3D mapping information puts all of the sci-

ence analyses to date into geologic context on a daily basis instead of weeks or months, as was the norm prior to this contribution. This allows the science planners to judge the efficacy of their previously executed science observations much more efficiently, and achieve greater science return as a result.

The Interactive 3D Mars surface view is a Mars terrain browsing software interface that encompasses the entire region of exploration for a Mars surface exploration mission. The view is interactive, allowing the user to pan in any direction by clicking and dragging, or to zoom in or out by scrolling the mouse or touchpad. This set currently includes tools for selecting a point of interest, and a ruler tool for displaying the distance between and positions of two points of interest.

The mapping information can be harvested and shared through ubiquitous online mapping tools like Google Mars, NASA WorldWind, and World-wide Telescope.

*This work was done by Mark W. Powell of Caltech for NASA's Jet Propulsion Laboratory. Further information is contained in a TSP (see page 1).*

*This software is available for commercial licensing. Please contact Daniel Broderick of the California Institute of Technology at [danielb@caltech.edu](mailto:danielb@caltech.edu). Refer to NPO-47311.*

---

## Rapid Diagnostics of Onboard Sequences

Keeping track of sequences onboard a spacecraft is challenging. When reviewing Event Verification Records (EVRs) of sequence executions on the Mars Exploration Rover (MER), operators often found themselves wondering which version of a named sequence the EVR corresponded to. The lack of this information drastically impacts the operators' diagnostic capabilities as well as their situational awareness with respect to the commands the spacecraft has executed, since the EVRs do not provide argument values or explanatory comments. Having this information immediately available can be instrumental in diagnosing critical events and can significantly enhance the overall safety of the spacecraft.

This software provides auditing capability that can eliminate that uncertainty while diagnosing critical conditions. Furthermore, the Restful interface provides a simple way for sequencing tools to automatically retrieve binary compiled sequence SCMFs (Space Com-

mand Message Files) on demand. It also enables developers to change the underlying database, while maintaining the same interface to the existing applications. The logging capabilities are also beneficial to operators when they are trying to recall how they solved a similar problem many days ago: this software enables automatic recovery of SCMF and RML (Robot Markup Language) sequence files directly from the command EVRs, eliminating the need for people to find and validate the corresponding sequences.

To address the lack of auditing capability for sequences onboard a spacecraft during earlier missions, extensive logging support was added on the Mars Science Laboratory (MSL) sequencing server. This server is responsible for generating all MSL binary SCMFs from RML input sequences. The sequencing server logs every SCMF it generates into a MySQL database, as well as the high-level RML file and dictionary name inputs used to create the SCMF. The SCMF is then indexed by a hash value that is automatically included in all command EVRs by the onboard flight software. Second, both the binary SCMF result and the RML input file can be retrieved simply by specifying the hash to a Restful web interface. This interface enables command line tools as well as large sophisticated programs to download the SCMF and RMLs on-demand from the database, enabling a vast array of tools to be built on top of it. One such command line tool can retrieve and display RML files, or annotate a list of EVRs by interleaving them with the original sequence commands.

This software has been integrated with the MSL sequencing pipeline where it will serve sequences useful in diagnostics, debugging, and situational awareness throughout the mission.

*This work was done by Thomas W. Starbird, John R. Morris, Khawaja S. Shams, and Mark W. Maimone of Caltech for NASA's Jet Propulsion Laboratory. For more information, contact [iaoffice@jpl.nasa.gov](mailto:iaoffice@jpl.nasa.gov).*

*This software is available for commercial licensing. Please contact Daniel Broderick of the California Institute of Technology at [danielb@caltech.edu](mailto:danielb@caltech.edu). Refer to NPO-48080.*

---

## MER Telemetry Processor

MERTELEMPROC processes telemetered data in data product format and generates Experiment Data Records (EDRs) for many instruments (HAZCAM, NAVCAM, PANCAM, microscopic imager, Mössbauer spectrometer, APXS, RAT, and EDLCAM) on the Mars Exploration Rover (MER). If the data is compressed, then MERTELEMPROC decompresses the data with an appropriate decompression algorithm. There are two compression algorithms (ICER and LOCO) used in MER. This program fulfills a MER specific need to generate Level 1 products within a 60-second time requirement.

EDRs generated by this program are used by `merinverter`, `marscahv`, `marsrad`, and `marsjplstereo` to generate higher-level products for the mission operations. MERTELEMPROC was the first GDS program to process the data product. Metadata of the data product is in XML format. The software allows user-configurable input parameters, per-product processing (not stream-based processing), and fail-over is allowed if the leading image header is corrupted. It is used within the MER automated pipeline.

MERTELEMPROC is part of the OPGS (Operational Product Generation Subsystem) automated pipeline, which analyzes images returned by in situ spacecraft and creates level 1 products to assist in operations, science, and outreach.

*This work was done by Hyun H. Lee of Caltech for NASA's Jet Propulsion Laboratory. For more information, contact [iaoffice@jpl.nasa.gov](mailto:iaoffice@jpl.nasa.gov).*

*This software is available for commercial licensing. Please contact Daniel Broderick of the California Institute of Technology at [danielb@caltech.edu](mailto:danielb@caltech.edu). Refer to NPO-47797.*

---

## pyam: Python implementation of YaM

pyam is a software development framework with tools for facilitating the rapid development of software in a concurrent software development environment. pyam provides solutions for devel-

opment challenges associated with software reuse, managing multiple software configurations, developing software product lines, and multiple platform development and build management. pyam uses release-early, release-often development cycles to allow developers to integrate their changes incrementally into the system on a continual basis. It facilitates the creation and merging of branches to support the isolated development of immature software to avoid impacting the stability of the development effort. It uses modules and packages to organize and share software across multiple software products, and uses the concepts of link and work modules to reduce sandbox setup times even when the code-base is large. One side-benefit is the enforcement of a strong module-level encapsulation of a module's functionality and interface. This increases design transparency, system stability, and software reuse.

pyam is written in Python and is organized as a set of utilities on top of the open source SVN software version control package. All development software is organized into a collection of "modules." pyam "packages" are defined as sub-collections of the available modules. Developers can set up private sandboxes for module/package development. All module/package development takes place on private SVN branches. High-level pyam commands support the setup, update, and release of modules and packages. Released and pre-built versions of modules are available to developers. Developers can tailor the source/link module mix for their sandboxes so that new sandboxes (even large ones) can be built up easily and quickly by pointing to pre-existing module releases. All inter-module interfaces are publicly exported via links. A minimal, but uniform, convention is used for building modules.

*This work was done by Steven Myint and Abhinandan Jain of Caltech for NASA's Jet Propulsion Laboratory. For more information, contact [iaoffice@jpl.nasa.gov](mailto:iaoffice@jpl.nasa.gov).*

*This software is available for commercial licensing. Please contact Daniel Broderick of the California Institute of Technology at [danielb@caltech.edu](mailto:danielb@caltech.edu). Refer to NPO-48447.*





## Process for Patterning Indium for Bump Bonding

*Goddard Space Flight Center, Greenbelt, Maryland*

An innovation was created for the Cosmology Large Angular Scale Surveyor for integration of low-temperature detector chips with a silicon backshort and a silicon photonic choke through flip-chip bonding. Indium bumps are typically patterned using liftoff processes, which require thick resist. In some applications, it is necessary to locate the bumps close to high-aspect-ratio structures such as wafer through-holes. In those cases, liftoff processes are challenging, and require complicated and time-consuming spray coating technology if the high-aspect-ratio structures are

delineated prior to the indium bump process. Alternatively, processing the indium bumps first is limited by compatibility of the indium with subsequent processing. The present invention allows for locating bumps arbitrarily close to multiple-level high-aspect-ratio structures, and for indium bumps to be formed without liftoff resist.

The process uses the poor step coverage of indium deposited on a silicon wafer that has been previously etched to delineate the location of the indium bumps. The silicon pattern can be processed through standard lithogra-

phy prior to adding the high-aspect-ratio structures. Typically, high-aspect-ratio structures require a thick resist layer so this layer can easily cover the silicon topography. For multiple levels of topography, the silicon can be easily conformally coated through standard processes. A blanket layer of indium is then deposited onto the full wafer; bump bonding only occurs at the high points of the topography.

*This work was done by Kevin Denis of Goddard Space Flight Center. Further information is contained in a TSP (see page 1). GSC-16386-1*

## Archway for Radiation and Micrometeorite Occurrence Resistance

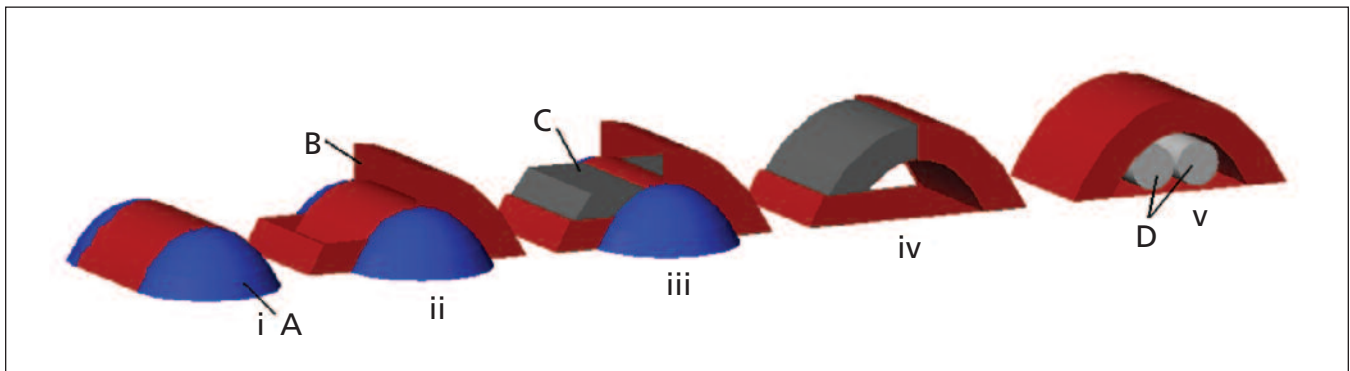
**This technology can be used where there is a need to rapidly deploy large, rugged structures including military, emergency services and disaster relief, and camping.**

*NASA's Jet Propulsion Laboratory, Pasadena, California*

The environmental conditions of the Moon require mitigation if a long-term human presence is to be achieved for extended periods of time. Radiation, micrometeoroid impacts, high-velocity debris, and thermal cycling represent threats to crew, equipment, and facilities. For decades, local regolith has been suggested as a candidate material to use in the construction of protective barriers. A thickness of roughly 3 m is

sufficient protection from both direct and secondary radiation from cosmic rays and solar protons; this thickness is sufficient to reduce radiation exposure even during solar flares. NASA has previously identified a need for innovations that will support lunar habitats using lightweight structures because the reduction of structural mass translates directly into additional up and down mass capability that would facilitate addi-

tional logistics capacity and increased science return for all mission phases. The development of non-pressurized primary structures that have synergy with the development of pressurized structures is also of interest. The use of indigenous or in situ materials is also a well-known and active area of research that could drastically improve the practicality of human exploration beyond low-Earth orbit.



**Views of ARMOR Construction.** The temporary inflatable (A) deploys (i). Then the jacket (B) is deployed (ii). Regolith (C) is then poured into the jacket and initially supported by the inflatable (iii). When the jacket is filled, the regolith inside the arch of the jacket is self-supporting, and the inflatable is no longer necessary (iv). Habitat modules and equipment (D) can be moved into the ARMOR (v). The jacket is shown in cutaway in steps (ii), (iii), and (iv) to illustrate regolith filling.

The Archway for Radiation and Micrometeorite Occurrence Resistance (ARMOR) concept is a new, multifunctional structure that acts as radiation shielding and micrometeorite impact protection for long-duration lunar surface protection of humans and equipment. ARMOR uses a combination of native regolith and a deployed membrane “jacket” to yield a multifunctional structure. ARMOR is a robust and modular system that can be autonomously assembled on-site prior to the first human surface arrival.

The system provides protection by holding a sufficiently thick (3 m) arch-shaped shell of local regolith around a central cavity. The regolith is held in shape by an arch-shaped jacket made of strong but deployable material. No re-

golith processing is required. During the regolith filling process, an inflatable structure under the arch supports the mass of the regolith, but once regolith filling is complete the catenary arch formed by the regolith and the jacket becomes self-supporting and the inflatable can be deflated and removed. When complete, habitat modules and equipment can be moved into the protected cavity under the arch. ARMOR is a near-term system that would provide a reliable and robust lightweight structure technology to support large lunar habitats, drastically lower launch mass, and improve efficient volume use, reducing launch costs.

ARMOR also protects from micrometeorites. The kinetic energy of micrometeorites and other debris will be ab-

sorbed first by an external, high-strength blanket held over and slightly away from the ARMOR jacket. The projectile penetrates this outer blanket, but becomes fragmented and loses energy in the process. The remnants of the projectile then impact the exterior of the jacket, and the jacket and regolith absorb the remaining kinetic energy. Facilities placed inside the ARMOR will be protected from direct sunlight, reducing the extreme temperature variations. Infrared radiation from the facility will be reflected by the interior of the ARMOR back onto the facility, reducing heat loss.

*This work was done by Dr. Louis R. Giersch of Caltech for NASA's Jet Propulsion Laboratory. Further information is contained in a TSP (see page 1). NPO-47686*





## 4D Light Field Imaging System Using Programmable Aperture

This system would be useful for inspections and surgeries, as well as in any stereo imaging system using two cameras.

NASA's Jet Propulsion Laboratory, Pasadena, California

Complete depth information can be extracted from analyzing all angles of light rays emanated from a source. However, this angular information is lost in a typical 2D imaging system. In order to record this information, a standard stereo imaging system uses two cameras to obtain information from two view angles. Sometimes, more cameras are used to obtain information from more angles. However, a 4D light field imaging technique can achieve this multiple-camera effect through a single-lens camera.

Two methods are available for this: one using a microlens array, and the other using a moving aperture. The moving-aperture method can obtain more complete stereo information. The existing literature suggests a modified liquid crystal panel [LC (liquid crystal)

panel, similar to ones commonly used in the display industry] to achieve a moving aperture. However, LC panels cannot withstand harsh environments and are not qualified for spaceflight. In this regard, different hardware is proposed for the moving aperture.

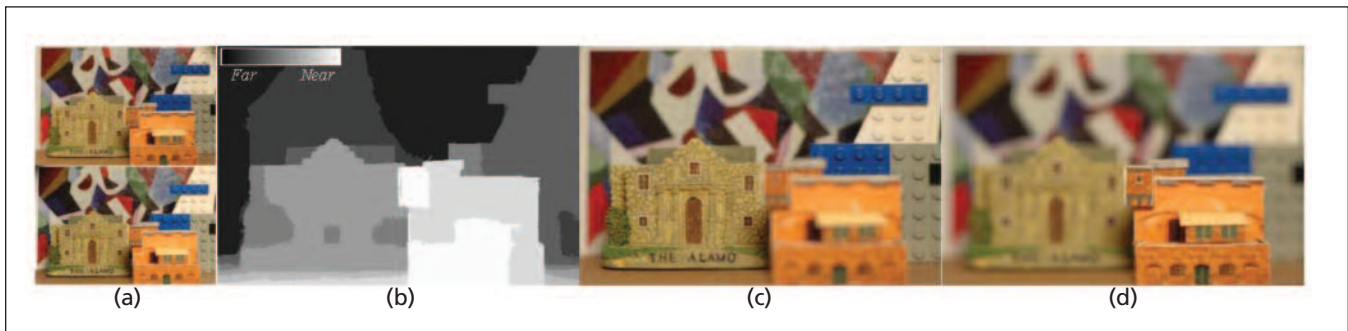
A digital micromirror device (DMD) will replace the liquid crystal. This will be qualified for harsh environments for the 4D light field imaging. This will enable an imager to record near-complete stereo information.

The approach to building a proof-of-concept is using existing, or slightly modified, off-the-shelf components. An SLR (single-lens reflex) lens system, which typically has a large aperture for fast imaging, will be modified. The lens system will be arranged so that DMD can be integrated. The shape of aperture will

be programmed for single-viewpoint imaging, multiple-viewpoint imaging, and coded aperture imaging.

The novelty lies in using a DMD instead of a LC panel to move the apertures for 4D light field imaging. The DMD uses reflecting mirrors, so any light transmission lost (which would be expected from the LC panel) will be minimal. Also, the MEMS-based DMD can withstand higher temperature and pressure fluctuation than a LC panel can. Robotics need near complete stereo images for their autonomous navigation, manipulation, and depth approximation. The imaging system can provide visual feedback.

*This work was done by Youngsam Bae of Caltech for NASA's Jet Propulsion Laboratory. Further information is contained in a TSP (see page 1). NPO-48604*



(a) Two demultiplexed light field images generated by the 4D Light Field Imaging System. The full 4D resolution is  $4 \times 4 \times 3039 \times 2014$ . (b) The estimated depth map of the top image of (a). (c, d) Post-exposure refocused images generated from the light field and the depth maps.

## Device and Container for Reheating and Sterilization

This device can be used for packaged products that require heating prior to use.

Lyndon B. Johnson Space Center, Houston, Texas

Long-duration space missions require the development of improved foods and novel packages that do not represent a significant disposal issue. In addition, it would also be desirable if rapid heating technologies could be used on Earth as well, to improve food quality during a sterilization process. For this purpose, a

package equipped with electrodes was developed that will enable rapid reheating of contents via ohmic heating to serving temperature during space vehicle transit. Further, the package is designed with a resealing feature, which enables the package, once used, to contain and sterilize waste, including

human waste for storage prior to jettison during a long-duration mission.

Ohmic heating is a technology that has been investigated on and off for over a century. Literature indicates that foods processed by ohmic heating are of superior quality to their conventionally processed counterparts. This is due to

the speed and uniformity of ohmic heating, which minimizes exposure of sensitive materials to high temperatures. In principle, the material may be heated rapidly to sterilization conditions, cooled rapidly, and stored.

The ohmic heating device herein is incorporated within a package. While this by itself is not novel, a reusable feature also was developed with the intent that waste may be stored and re-sterilized within the packages. These would then serve a useful function after their use in food processing and storage.

The enclosure should be designed to minimize mass (and for NASA's purposes, Equivalent System Mass, or ESM), while enabling the sterilization function. It should also be electrically insulating. For this reason, Ultem® high-strength, machinable electrical insulator was used.

Because the pouch would expand

when exposed to heating to sterilization temperatures (greater than 121 °C), it is necessary to prevent seal rupture by applying air pressure into the enclosure. To enable cooling of the package in the enclosure, a water inlet and outlet are provided. The electrode tabs could be modified to form a larger pair of electrodes, which will also allow heating of water within the enclosure if necessary.

Under normal reheating conditions, temperatures will not need to go above 100 °C, thus the air overpressure feature will be unnecessary. The plan is to provide a user interface with a keypad that will enable users to dial in the heating protocol depending on the product that is within the chamber. This feature could be automated.

The incidence of electrolysis will be minimized using a solid-state IGBT

power supply at 10 kHz. This is critical in a space application, since bubble formation at the electrodes can stop the heating unless electrolysis can be suppressed.

*This work was done by Sudhir K. Sastry, Brian F. Heskitt, Soojin Jun, Joseph E. Marcy, and Ritesh Mahna of Ohio State University for Johnson Space Center. For further information, contact the JSC Innovation Partnerships Office at (281) 483-3809.*

*In accordance with Public Law 96-517, the contractor has elected to retain title to this invention. Inquiries concerning rights for its commercial use should be addressed to:*

*Office of Technology Licensing  
1960 Kenny Road 2nd floor  
Columbus, OH 43210-1063  
Phone No.: (614) 292-1315*

*Refer to MSC-23999-1, volume and number of this NASA Tech Briefs issue, and the page number.*

## Radio Frequency Plasma Discharge Lamps for Use as Stable Calibration Light Sources

**Electrode-induced instabilities are eliminated and the lifetime is not limited by electrode erosion.**

*Goddard Space Flight Center, Greenbelt, Maryland*

Stable high radiance in visible and near-ultraviolet wavelengths is desirable for radiometric calibration sources. In this work, newly available electrodeless radio-frequency (RF) driven plasma light sources were combined with research-grade, low-noise power supplies and coupled to an integrating sphere to produce a uniform radiance source. The stock light sources consist of a 28 VDC power supply, RF driver, and a resonant RF cavity. The RF cavity includes a small bulb with a fill gas that is ionized by the electric field and emits light. This assembly is known as the emitter. The RF driver supplies a source of RF energy to the emitter.

In commercial form, embedded electronics within the RF driver perform a continual optimization routine to maximize energy transfer to the emitter. This optimization routine continually varies the light output sinusoidally by approximately 2% over a several-second period. Modifying to eliminate this optimization eliminates the sinusoidal variation but allows the output to slowly drift over time. This drift can be minimized by allowing sufficient warm-up time to achieve thermal equilibrium. It was also found that supplying the RF driver with

a low-noise source of DC electrical power improves the stability of the lamp output. Finally, coupling the light into an integrating sphere reduces the effect of spatial fluctuations, and decreases noise at the output port of the sphere.

The RF-driven lamps have several advantages over traditional calibration sources. Currently, accurate radiance measurements can be made at infrared and the red portion of the visible wavelengths using tungsten filament-style FEL lamps. However, the blackbody output of these lamps is limited to 3,000 K, and intensity falls exponentially at shorter wavelengths at the blue end of the spectrum. For reproduction of the solar spectrum, with an equivalent blackbody temperature of 6000 K, the blue and ultraviolet wavelengths have typically been produced using high-pressure xenon arc discharge lamps. These lamps achieve the high temperature necessary in a narrow filament of ionized gas between two electrodes. This ion channel suffers from instabilities produced by buoyancy-induced turbulence of the surrounding gas. There is also longer-term drift associated with the sputtering of electrode material through ion impact, which changes both the electrode spacing

and surface profile. Due to the high electric field gradients, these small changes in geometry result in non-negligible changes to the light output.

Additionally, much of the sputtered electrode material is deposited as a thin layer on the inner surface of the lamp. This decreases light transmission through the glass and ultimately limits the useful life of the lamp to no more than 1,000 hours, over the course of which the radiant flux may decrease by a factor of two. Additionally, the xenon lamps generate several undesirable sharp emission lines with large intensity variation over a small spectral range. The electrode-induced instabilities are eliminated in the RF lamp, and the lifetime is not limited by electrode erosion. The higher operating pressure of the RF-driven bulbs produces a smoother broadband spectrum. The RF lamps are also more efficient, and have more conducive geometry for coupling their light into an integrating sphere.

*This work was done by Brendan McAndrew and John Cooper of Goddard Space Flight Center; and Angelo Arcchi, Greg McKee, and Christopher Durell of Labsphere, Inc. Further information is contained in a TSP (see page 1). GSC-16399-1*

## Membrane Shell Reflector Segment Antenna

**A tetrahedral truss provides rigidity and integrity for the reflector antenna.**

*NASA's Jet Propulsion Laboratory, Pasadena, California*

The mesh reflector is the only type of large, in-space deployable antenna that has successfully flown in space. However, state-of-the-art large deployable mesh antenna systems are RF-frequency-limited by both global shape accuracy and local surface quality. The limitations of mesh reflectors stem from two factors. First, at higher frequencies, the porosity and surface roughness of the mesh results in loss and scattering of the signal. Second, the mesh material does not have any bending stiffness and thus cannot be formed into true parabolic (or other desired) shapes.

To advance the deployable reflector technology at high RF frequencies from the current state-of-the-art, significant improvements need to be made in three major aspects: a high-stability and high-precision deployable truss; a continuously curved RF reflecting surface (the function of the surface as well as its first derivative are both continuous); and the RF reflecting surface should be made of a continuous material. To meet these three requirements, the Membrane

Shell Reflector Segment (MSRS) antenna was developed.

A MSRS antenna is composed of a deployable tetrahedral truss that supports a set of MSRSs to form a high-definition, smooth, and continuous surface. This high radio-frequency (RF) deployable reflector is implemented by leveraging and integrating several recently developed material technologies: shape memory polymer (SMP) composite material; high-precision MSRS casting process; near-zero coefficient of thermal expansion (CTE) membrane material; and poly-vinylidene fluoride (PVDF) electro-active membrane. This reflector technology can potentially offer almost one order of magnitude higher precision than current state-of-the-art reflectors, and can provide very complex reflector shapes.

The structural part of this MSRS antenna is a tetrahedral truss that provides rigidity and integrity for the reflector. Tetrahedral trusses offer much higher precision than tensioning cable

trusses that are employed by all current state-of-the-art mesh reflectors. However, it is extremely difficult to package a tetrahedral truss by using traditional deployment mechanisms. The unique characteristic of the SMP composite makes it possible to package and deploy the whole reflector. The fundamental requirement on a high RF reflector, high precision, will naturally be met by the intrinsic accuracy characteristic of the tetrahedral configuration. The high-definition RF reflective surface is composed of a number of MSRSs made of either near-zero CTE Novastrat or PVDF membrane. The thickness and curvature of each MSRS provide sufficient shell stiffness for it to be supported by the tetrahedral truss at three points.

*This work was done by Houfei Fang and Eastwood Im of Caltech, John Lin of ILC Dover LP, and Jim Moore of NeXolve Corporation for NASA's Jet Propulsion Laboratory. Further information is contained in a TSP (see page 1). NPO-48317*

## High-Speed Transport of Fluid Drops and Solid Particles via Surface Acoustic Waves

**The innovation can act as a bladeless wiper for raindrops.**

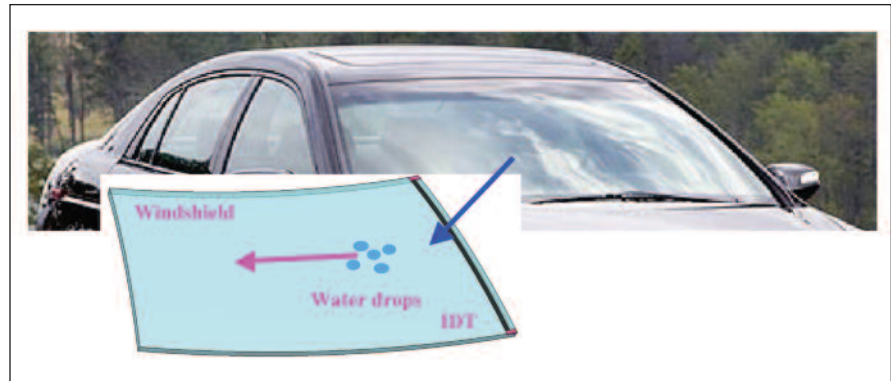
*NASA's Jet Propulsion Laboratory, Pasadena, California*

A compact sampling tool mechanism that can operate at various temperatures, and transport and sieve particle sizes of powdered cuttings and soil grains with no moving parts, has been created using traveling surface acoustic waves (SAWs) that are emitted by an inter-digital transducer (IDT). The generated waves are driven at about 10 MHz, and it causes powder to move towards the IDT at high speed with different speeds for different sizes of particles, which enables these particles to be sieved.

This design is based on the use of SAWs and their propelling effect on powder particles and fluids along the path of the waves. Generally, SAWs are elastic waves propagating in a shallow layer of about one wavelength beneath the surface of a solid substrate. To generate SAWs, a piezoelectric plate is used

that is made of  $\text{LiNbO}_3$  crystal cut along the  $x$ -axis with rotation of  $127.8^\circ$  along the  $y$ -axis. On this plate are printed pairs of fingerlike electrodes in the form of a grating that are activated by subjecting

the gap between the electrodes to electric field. This configuration of a surface wave transmitter is called IDT. The IDT that was used consists of 20 pairs of fingers with 0.4-mm spacing, a total length



An automobile windshield with an Inter-Digital Transducer is shown as a replacement for movable wiper blades.

of 12.5 mm. The surface wave is produced by the nature of piezoelectric material to contract or expand when subjected to an electric field.

Driving the IDT to generate wave at high amplitudes provides an actuation mechanism where the surface particles move elliptically, pulling powder particles on the surface toward the wave-source and pushing liquids in the opposite direction. This behavior allows the

innovation to separate large particles and fluids that are mixed. Fluids are removed at speed (7.5 to 15 cm/s), enabling this innovation of acting as a bladeless wiper for raindrops. For the windshield design, the electrodes could be made transparent so that they do not disturb the driver or pilot.

Multiple IDTs can be synchronized to transport water or powder over larger distances. To demonstrate the

transporting action, a video camera was used to record the movement. The speed of particles was measured from the video images.

*This work was done by Yoseph Bar-Cohen, Xiaoqi Bao, Stewart Sherrit, Mircea Badescu, and Shyh-shiuh Lih of Caltech for NASA's Jet Propulsion Laboratory. Further information is contained in a TSP (see page 1). NPO-46252*

## Compact Autonomous Hemispheric Vision System

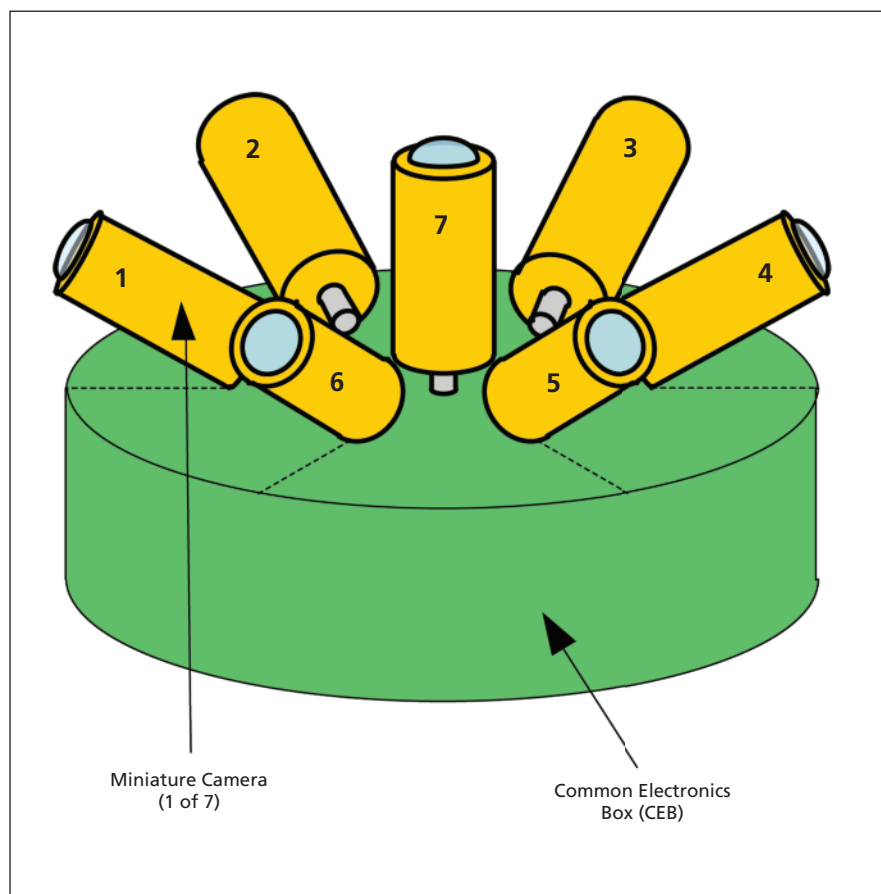
System has no moving parts and features expanded capabilities.

NASA's Jet Propulsion Laboratory, Pasadena, California

Solar System Exploration camera implementations to date have involved either single cameras with wide field-of-view (FOV) and consequently coarser spatial resolution, cameras on a movable mast, or single cameras necessitating rotation of the host vehicle to afford visibility outside a relatively narrow FOV. These cameras require detailed commanding from the ground or separate onboard computers to operate properly, and are incapable of making decisions based on image content that control pointing and downlink strategy. For color, a filter wheel having selectable positions was often added, which added moving parts, size, mass, power, and reduced reliability.

A system was developed based on a general-purpose miniature visible-light camera using advanced CMOS (complementary metal oxide semiconductor) imager technology. The baseline camera has a 92° FOV and six cameras are arranged in an angled-up carousel fashion, with FOV overlaps such that the system has a 360° FOV (azimuth). A seventh camera, also with a FOV of 92°, is installed normal to the plane of the other 6 cameras giving the system a >90° FOV in elevation and completing the hemispheric vision system. A central unit houses the common electronics box (CEB) controlling the system (power conversion, data processing, memory, and control software).

Stereo is achieved by adding a second system on a baseline, and color is achieved by stacking two more systems (for a total of three, each system equipped with its own filter.) Two connectors on the bottom of the CEB provide a connection to a carrier (rover,



View of the Baseline 7-Camera Concept (360° horizontal FOV, >90° vertical FOV)

spacecraft, balloon, etc.) for telemetry, commands, and power. This system has no moving parts.

The system's onboard software (SW) supports autonomous operations such as pattern recognition and tracking. For example, when the system is commanded to detect and track an object of interest, the SW continuously reads

data from all the cameras until the object appears in one (or more) camera's FOV. The SW then reads these camera(s) and only returns to Earth the portion of the data that includes the object of interest.

Each camera weighs 50 g, measures 2 cm in diameter, 4 cm in length, and consumes less than 50 mW. The central elec-

tronics is a cylinder 14 cm in diameter and 4 cm thick. Variations with different and smaller form factors are possible.

By using the massively parallel architecture inherent to field-programmable gate arrays (FPGAs), per-imager processing may be performed concurrently by separate computational units within the FPGA. This architecture allows tracking

algorithms to scan the entire FOV for a set of features and then switch to a second operating mode that performs processing targeted to only the imagers capturing those features. This architecture would provide considerable bonus to science by improving the efficiency of long-range survey with no additional mass and very small power cost.

*This work was done by Paula J. Pingree, Thomas J. Cunningham, Thomas A. Werne, Michael L. Eastwood, Marc J. Walch, and Robert L. Staehle of Caltech for NASA's Jet Propulsion Laboratory. For more information, contact iaoffice@jpl.nasa.gov. NPO-48172*

---

## A Distributive, Non-Destructive, Real-Time Approach to Snowpack Monitoring

*Goddard Space Flight Center, Greenbelt, Maryland*

This invention is designed to ascertain the snow water equivalence (SWE) of snowpacks with better spatial and temporal resolutions than present techniques. The approach is ground-based, as opposed to some techniques that are air-based. In addition, the approach is compact, non-destructive, and can be communicated with remotely, and thus can be deployed in areas not possible with current methods.

Presently there are two principal ground-based techniques for obtaining SWE measurements. The first is manual snow core measurements of the snow-

pack. This approach is labor-intensive, destructive, and has poor temporal resolution. The second approach is to deploy a large (e.g., 3×3 m) snowpillow, which requires significant infrastructure, is potentially hazardous [uses a ≈200-gallon (≈760-L) antifreeze-filled bladder], and requires deployment in a large, flat area. High deployment costs necessitate few installations, thus yielding poor spatial resolution of data. Both approaches have limited usefulness in complex and/or avalanche-prone terrains. This approach is compact, non-destructive to the snowpack, provides high

temporal resolution data, and due to potential low cost, can be deployed with high spatial resolution.

The invention consists of three primary components: a robust wireless network and computing platform designed for harsh climates, new SWE sensing strategies, and algorithms for smart sampling, data logging, and SWE computation.

*This work was done by Jeff Frolik and Christian Skalka of the University of Vermont for Goddard Space Flight Center. Further information is contained in a TSP (see page 1). GSC-16352-1*





### **Wideband Single-Crystal Transducer for Bone Characterization**

**These transducers have uses in medical ultrasound imaging and room-temperature ultrasonic flow meters.**

*John H. Glenn Research Center, Cleveland, Ohio*

The microgravity conditions of space travel result in unique physiological demands on the human body. In particular, the absence of the continual mechanical stresses on the skeletal system that are present on Earth cause the bones to decalcify. Trabecular structure decreases in thickness and increases in spacing, resulting in decreased bone strength and increased risk of injury. Thus, monitoring bone health is a high priority for long-term space travel. A single probe covering all frequency bands of interest would be ideal for such measurements, and this would also minimize storage space and eliminate the complexity of integrating multiple probes.

This invention is an ultrasound transducer for the structural characterization of bone. Such characterization measures features of reflected and transmitted ultrasound signals, and correlates these signals with bone structure metrics such as bone mineral density, trabecular spacing, and thickness, etc. The techniques used to determine these various metrics require measurements over a broad range of ultrasound frequencies, and therefore, complete characterization requires the use of several narrowband transducers.

This is a single transducer capable of making these measurements in all the

required frequency bands. The device achieves this capability through a unique combination of a broadband piezoelectric material; a design incorporating multiple resonator sizes with distinct, overlapping frequency spectra; and a micromachining process for producing the multiple-resonator pattern with common electrode surfaces between the resonators.

This device consists of a pattern of resonator bars with common electrodes that is wrapped around a central mandrel such that the radiating faces of the resonators are coplanar and can be simultaneously applied to the sample to be measured. The device operates as both a source and receiver of acoustic energy. It is operated by connection to an electronic system capable of both providing an excitation signal to the transducer and amplifying the signal received from the transducer. The excitation signal may be either a wide-bandwidth signal to excite the transducer across its entire operational spectrum, or a narrow-bandwidth signal optimized for a particular measurement technique. The transducer face is applied to the skin covering the bone to be characterized, and may be operated in through-transmission mode using two transducers, or in pulse-echo mode.

The transducer is a unique combination of material, design, and fabrication technique. It is based on single-crystal lead magnesium niobate lead titanate (PMN-PT) piezoelectric material. As compared to the commonly used piezoceramics, this piezocrystal has superior piezoelectric and elastic properties, which results in devices with superior bandwidth, source level, and power requirements. This design necessitates a single resonant frequency. However, by operating in a transverse length-extensional mode, with the electric field applied orthogonally to the extensional direction, resonators of different sizes can share common electrodes, resulting in a multiply-resonant structure. With carefully sized resonators, and the superior bandwidth of piezocrystal, the resonances can be made to overlap to form a smooth, wide-bandwidth characteristic.

*This work was done by Yu Liang and Kevin Snook of TRS Technologies, Inc. for Glenn Research Center. Further information is contained in a TSP (see page 1).*

*Inquiries concerning rights for the commercial use of this invention should be addressed to NASA Glenn Research Center, Innovative Partnerships Office, Attn: Steven Fedor, Mail Stop 4-8, 21000 Brookpark Road, Cleveland, Ohio 44135. Refer to LEW-18842-1.*







## Σ Numerical Simulation of Rocket Exhaust Interaction With Lunar Soil

**These simulations will help predict suitable landing sites on the Moon.**

*John F. Kennedy Space Center, Florida*

This technology development originated from the need to assess the debris threat resulting from soil material erosion induced by landing spacecraft rocket plume impingement on extraterrestrial planetary surfaces. The impact of soil debris was observed to be highly detrimental during NASA's Apollo lunar missions and will pose a threat for any future landings on the Moon, Mars, and other exploration targets.

The innovation developed under this program provides a simulation tool that combines modeling of the diverse disciplines of rocket plume impingement gas dynamics, granular soil material liberation, and soil debris particle kinetics into one unified simulation system. The Unified Flow Solver (UFS) developed by CFDRC enabled the efficient, seamless simulation of mixed continuum and rarefied rocket plume flow utilizing a novel direct numerical simulation technique of the Boltzmann gas dynamics equation. The characteristics of the soil granular material response and modeling of the erosion and liberation processes were enabled through novel first principle-based granular mechanics models developed by the University of Florida specifically for the highly irregularly shaped and co-

hesive lunar regolith material. These tools were integrated into a unique simulation system that accounts for all relevant physics aspects: (1) Modeling of spacecraft rocket plume impingement flow under lunar vacuum environment resulting in a mixed continuum and rarefied flow; (2) Modeling of lunar soil characteristics to capture soil-specific effects of particle size and shape composition, soil layer cohesion and granular flow physics; and (3) Accurate tracking of soil-borne debris particles beginning with aerodynamically driven motion inside the plume to purely ballistic motion in lunar far field conditions.

In the earlier project phase of this innovation, the capabilities of the UFS for mixed continuum and rarefied flow situations were validated and demonstrated for lunar lander rocket plume flow impingement under lunar vacuum conditions. Applications and improvements to the granular flow simulation tools contributed by the University of Florida were tested against Earth environment experimental results. Requirements for developing, validating, and demonstrating this solution environment were clearly identified, and an effective second phase execution plan was

devised. In this phase, the physics models were refined and fully integrated into a production-oriented simulation tool set. Three-dimensional simulations of Apollo Lunar Excursion Module (LEM) and Altair landers (including full-scale lander geometry) established the practical applicability of the UFS simulation approach and its advanced performance level for large-scale realistic problems.

The features and benefits of the developed simulation system enable the screening of landing risk scenarios through: identification of dust and debris transport footprint to protect surrounding assets; prediction of level of erosion and cratering as a function of rocket size and of local soil properties; input into the design of landing pad solidification or paving techniques; minimization of debris environment through optimization of propulsion system layout and landing approach flight path; and designing dust and debris impact mitigation measures such as berms, deflectors, and fences.

*This work was done by Peter Liever and Abhijit Tosh of CFD Research Corporation and Jennifer Curtis of the University of Florida for Kennedy Space Center. Further information is contained in a TSP (see page 1). KSC-13605*

## Σ Motion Imagery and Robotics Application (MIRA): Standards-Based Robotics

**MIRA initial results have demonstrated robotic camera control that is applicable to near-Earth or distant applications.**

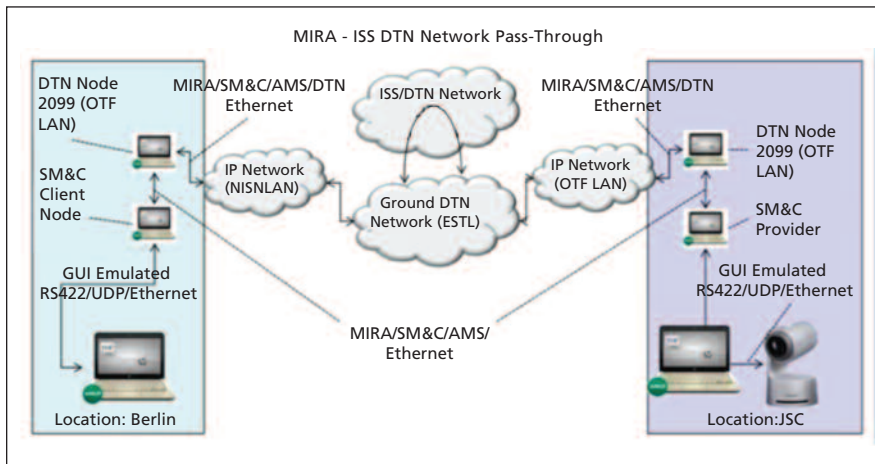
*Lyndon B. Johnson Space Center, Houston, Texas*

The current Mission Control Center (MCC) is dedicated to the execution of human spaceflight missions. As the future of NASA and human space evolves, it is clear that robotic artifacts will ultimately be integrated and immersed into the human mission. In order to make the evolution and integration as technically capa-

ble at a constrained risk level and with reasonable cost, the robotic elements must adhere to standards that allow not only reuse of previous work, but keep the interfaces stable and reusable.

The MIRA project integrates several telerobotic functions into a powerful Consultative Committee for Space Data

Systems (CCSDS) international standards-based telerobotic service capable of running in an International Space Station (ISS) payload computer. The MIRA goal was to mature, integrate, and demonstrate the MIRA concept (see figure), with Spacecraft Monitoring and Control (SM&C), Asynchronous Mes-



MIRA Architecture

saging Service (AMS), and the Delay Tolerant Network (DTN) standards into a single integrated protocol system.

The ultimate goal of the MIRA project is to develop an application stack for all robotics, even complex ones. It will be capable of status and control of three different cameras on the Exposed Facility (the porch) of the ISS JEM Module from MCC. Each successive phase will add incremental capabilities such as the capability of handling Human Factors and Performance (HFP), and automatic/semiautomatic change detection from imagery of spaceflight vehicles and equip-

ment. In later project phases, it will include ground control of robotic assets over Earth-Moon-Mars time delays, and remote sensing of planetary surfaces and surface navigation.

This project seeks to develop a new standard for robotics such that interoperability with crewed as well as non-crewed elements is provided, assuring cost effective collaboration between NASA and the international space community. The evolution of the proposed standard will be coordinated through the CCSDS International Standards community. The confluence of the

MIRA, SM&C/AMS/DTN standards, the robustness of DTN capability, and remote connectivity to ISS and ground assets (interoperability) will assure the JSC/MCC will be the hub of human, human precursor, and robotic missions where the mission components can be seamlessly integrated with other locations without excessive reconfiguration and integration costs that would render the MCC non-competitive.

The MIRA initial results have demonstrated robotic camera control that is applicable to near-Earth or distant applications where the DTN provides the bridge across the time delay impacts. The MIRA, SM&C/AMS/DTN standards-based status and control system software and protocol could be hardened, and expanded into the next-generation MCC protocol supporting human, robotic, and human-robotic missions. As such, this simple robotic camera prototype is a significant first step in the integration of robotic and human missions into true distant independent building blocks for future missions.

*This work was done by Lindolfo Martinez, Thomas Rich, Steven Lucord, Thomas Diegelman, James Mireles, and Pete Gonzalez of Johnson Space Center. Further information is contained in a TSP (see page 1). MSC-25164-1*

## Particle Filtering for Model-Based Anomaly Detection in Sensor Networks

Experiments on test stand sensor data show successful detection of a known anomaly in the test data.

*Stennis Space Center, Mississippi*

A novel technique has been developed for anomaly detection of rocket engine test stand (RETS) data. The objective was to develop a system that post-processes a csv file containing the sensor readings and activities (time-series) from a rocket engine test, and detects any anomalies that might have occurred during the test. The output consists of the names of the sensors that show anomalous behavior, and the start and end time of each anomaly.

In order to reduce the involvement of domain experts significantly, several data-driven approaches have been proposed where models are automatically acquired from the data, thus bypassing the cost and effort of building system

models. Many supervised learning methods can efficiently learn operational and fault models, given large amounts of both nominal and fault data. However, for domains such as RETS data, the amount of anomalous data that is actually available is relatively small, making most supervised learning methods rather ineffective, and in general met with limited success in anomaly detection.

The fundamental problem with existing approaches is that they assume that the data are iid, i.e., independent and identically distributed, which is violated in typical RETS data. None of these techniques naturally exploit the temporal information inherent in time series data

from the sensor networks. There are correlations among the sensor readings, not only at the same time, but also across time. However, these approaches have not explicitly identified and exploited such correlations. Given these limitations of model-free methods, there has been renewed interest in model-based methods, specifically graphical methods that explicitly reason temporally. The Gaussian Mixture Model (GMM) in a Linear Dynamic System approach assumes that the multi-dimensional test data is a mixture of multi-variate Gaussians, and fits a given number of Gaussian clusters with the help of the well-known Expectation Maximization (EM) algorithm. The parameters thus learned

are used for calculating the joint distribution of the observations. However, this GMM assumption is essentially an approximation and signals the potential viability of non-parametric density estimators. This is the key idea underlying the new approach.

Since this approach was model-based, it was possible to automatically learn a model of nominal behavior from tests that were marked nominal. Particle filtering and machine learning were applied to capture the model of nominal operations, and voting techniques were used in conjunction with particle filter-

ing to detect anomalies in test runs. Experiments on test stand sensor data show successful detection of a known anomaly in the test data, while producing almost no false positives.

A novel combination of particle filtering, machine learning, and voting techniques was developed to detect anomalies in sensor network data. Although most of the subsystems are tightly integrated into the system, the following two subsystems can also be used as standalone for extraneous tasks. A novel, efficient (but approximate) correlation clustering method that is currently used for sensor

selection was developed, but it can also be used to visualize sensor correlations as an aid to manual analysis. Sensors are detected that are overactive (large variance) or underactive (low variance) between commands, which effectively give a high-level map of the effect of commands on sensor groups. This may be used as an aid to visual/manual analysis.

*This work was done by Wanda Solano of Stennis Space Center, and Bikramjit Banerjee and Landon Kraemer of The University of Southern Mississippi. For more information, call the SSC Center Chief Technologist at 228-688-1929. Refer to SSC-00379.*





## Books & Reports

### **Ka-band Digitally Beam-formed Airborne Radar Using SweepSAR Technique**

A paper describes a frequency-scaled SweepSAR demonstration that operates at Ka-Band (35.6 GHz), and closely approximates the DESDynI mission antenna geometry, scaled by 28. The concept relies on the SweepSAR measurement technique. An array of digital receivers captures waveforms from a multiplicity of elements. These are combined using digital beamforming in elevation and SAR processing to produce imagery.

Ka-band (35.6 GHz) airborne SweepSAR using array-fed reflector and digital beamforming features eight simultaneous receive beams generated by a 40-cm offset-fed reflector and eight-element active array feed, and eight digital receiver channels with all raw data recorded and later used for beamforming. Illumination of the swath is accomplished using a slotted-waveguide antenna radiating 250 W peak power. This experiment has been used to demonstrate digital beamforming SweepSAR systems.

*This work was done by Gregory A. Sadowy, Chung-Lun Chuang, Hiran Ghaemi, Brandon A. Heavey, Lung-Sheng S. Lin, and Momin Qudus of Caltech for NASA's Jet Propulsion Laboratory. Further information is contained in a TSP (see page 1). NPO-48376*

### **Composite With In Situ Plenums**

A document describes a high-performance thermal distribution panel (TDP) concept using high-conductivity (>800 W/mK) macro composite skin with *in situ* heat pipes. The processing technologies proposed to build such a panel result in a one-piece, inseparable assembly with high conductance in both the X and Y planes. The TDP configuration can also be used to produce panels with high structural stiffness. The one-piece construction of the TDP eliminates the thermal interface between the cooling plenums and the heat spreader base, and obviates the need for bulky mounting flanges and thick heat spreaders used on baseline designs. The conductivity of the TDP can be configured to exceed 800 W/mK with a mass density below 2.5 g/cm<sup>3</sup>. This material can provide efficient conductive heat transfer between the *in situ* heat plenums, permitting the use of thinner panel thicknesses. The

plenums may be used as heat pipes, loop heat pipes, or liquid cooling channels.

The panel technology used in the TDP is a macro-composite comprised of aluminum-encapsulated annealed pyrolytic graphite (APG). APG is highly aligned crystalline graphite with an in-plane thermal conductivity of 1,700 W/mK. APG has low shear strength and does not constrain the encapsulating material.

The proposed concept has no thermal interfaces between the heat pipes and the spreader plate, further improving the overall conductance of the system. The *in situ* plenums can also be used for liquid cooling applications. The process can be used to fabricate structural panels by adding a second thin sheet.

*This work was done by Mark Montesano of k-Technology, a Division of Thermacore, for Goddard Space Flight Center. Further information is contained in a TSP (see page 1). GSC-16043-1*

### **Multi-Beam Approach for Accelerating Alignment and Calibration of HypSIRI-Like Imaging Spectrometers**

A paper describes an optical stimulus that produces more consistent results, and can be automated for unattended, routine generation of data analysis products needed by the integration and testing team assembling a high-fidelity imaging spectrometer system. One key attribute of the system is an arrangement of pick-off mirrors that provides multiple input beams (five in this implementation) to simultaneously provide stimulus light to several field angles along the field of view of the sensor under test, allowing one data set to contain all the information that previously required five data sets to be separately collected. This stimulus can also be fed by quickly reconfigured sources that ultimately provide three data set types that would previously be collected separately using three different setups: Spectral Response Function (SRF), Cross-track Response Function (CRF), and Along-track Response Function (ARF), respectively.

This method also lends itself to expansion of the number of field points if less interpolation across the field of view is desirable. An absolute minimum of three is required at the beginning stages of imaging spectrometer alignment.

*This work was done by Michael L. Eastwood,*

*Robert O. Green, Pantazis Mowoulis, Eric B. Hochberg, Randall C. Hein, Linley A. Kroll, Sven Geier, and James B. Coles of Caltech, and Riley Meehan of Tufts University for NASA's Jet Propulsion Laboratory. Further information is contained in a TSP (see page 1). NPO-47809*

### **JWST Lifting System**

A document describes designing, building, testing, and certifying a customized crane (Lifting Device — LD) with a strong back (cradle) to facilitate the installation of long wall panels and short door panels for the GHe phase of the James Webb Space Telescope (JWST).

The LD controls are variable-frequency drive controls designed to be adjustable for very slow and very-short-distance movements throughout the installation. The LD has a lift beam with an electric actuator attached at the end. The actuator attaches to a rectangular strong back (cradle) for lifting the long wall panels and short door panels from a lower angle into the vertical position inside the chamber, and then rotating around the chamber for installation onto the existing ceiling and floor.

The LD rotates 360° (in very small increments) in both clockwise and counter-clockwise directions. Eight lifting pads are on the top ring with 2-in. (≈5-cm) eye holes spaced evenly around the ring to allow for the device to be suspended by three crane hoists from the top of the chamber.

The LD is operated by remote controls that allow for a single, slow mode for booming the load in and out, with slow and very slow modes for rotating the load.

*This work was done by William Tolleson of CSC Applied Technologies LLC for Johnson Space Center. Further information is contained in a TSP (see page 1). MSC-25176-1*

### **Next-Generation Tumbleweed Rover**

A document describes a next-generation tumbleweed rover that involves a split balloon system that is made up of two half-spherical air bladders with a disc between them. This disc contains all the electronics and instruments. By deflating only the bottom balloon, the rover can sit, bringing the surface probe into contact with the ground. The bottom balloon has a channel passing through it, allowing the surface probe to reach the surface through the balloon.

Once the sample has been gathered and analyzed, the rover can re-inflate the lower air bladder and continue rolling.

The rover will use a small set of instruments and electronics situated at the center of its inflatable spherical hull. The current version is a large beach-ball-like construction, about 1.8 m in diameter and weighing roughly 15 kg. The rover comprises two major parts, an outer spherical hull (split in half at the central disc) and an inner, disc-shaped cylindrical section. The balloons are attached to the bottom and top of the disc. Inside the disc, there are temperature and pressure sensors to keep track of the inner and outer conditions of the rover. A system of pumps and valves is responsible for independently inflating and deflating the balloons as necessary. There are also accelerometers to record the movement, together with a GPS receiver. The data are then sent through a modem to a con-

trol station. This work builds upon the project "Tumbleweed rover for planetary exploration," described in the Technical Support Package, as noted below.

*This work was done by Jeffrey P. Nosanov of Caltech for NASA's Jet Propulsion Laboratory. Further information is contained in a TSP (see page 1). NPO-47648*

---

### **Pneumatic System for Concentration of Micrometer-Size Lunar Soil**

A report describes a size-sorting method to separate and concentrate micrometer-size dust from a broad size range of particles without using sieves, fluids, or other processes that may modify the composition or the surface properties of the dust.

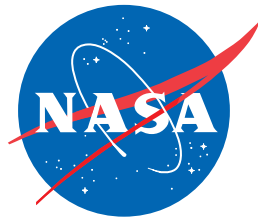
The system consists of four processing units connected in series by tubing. Samples of dry particulates such as lunar soil

are introduced into the first unit, a fluidized bed. The flow of introduced nitrogen fluidizes the particulates and preferentially moves the finer grain sizes on to the next unit, a flat plate impactor, followed by a cyclone separator, followed by a Nuclepore polycarbonate filter to collect the dust.

By varying the gas flow rate and the sizes of various orifices in the system, the size of the final and intermediate particles can be varied to provide the desired products. The dust can be collected from the filter. In addition, electron microscope grids can be placed on the Nuclepore filter for direct sampling followed by electron microscope characterization of the dust without further handling.

*This work was done by David McKay and Bonnie Cooper of Johnson Space Center. Further information is contained in a TSP (see page 1). MSC-25264-1*





National Aeronautics and  
Space Administration